

Growth of Alkali Halides from Molecular Beams: Global Growth Characteristics

M. H. Yang and C. P. Flynn

*Department of Physics and the Materials Research Laboratory, University of Illinois at Urbana-Champaign,
1110 West Green Street, Urbana, Illinois 61801*

(Received 7 February 1989)

Alkali-halide single crystals are shown to grow from molecular beams under conditions systematically different from those for metals and elemental semiconductors, for reasons related to ionic bonding. Heteroepitaxy and the occurrence of epitaxially stabilized new alkali-halide alloys and compounds are discussed.

PACS numbers: 61.50.Cj, 68.55.Bd, 81.20.Lb

The conditions under which materials can be grown by molecular-beam epitaxy (MBE) depend markedly on the type of crystal cohesion. For example, metal heterojunctions grown by MBE on nonvicinal surfaces, and at ordinary rates $\sim 1 \text{ \AA}/\text{sec}$, have smooth sharp interfaces only at growth temperature $T_g \sim 3T_m/8$, with T_m the (absolute) melting temperature.¹ This optimum arises from the following:² (i) the fast surface diffusion, D_s , required to precipitate all incident species on existing ledges, thereby inhibiting nucleation of new ledges and hence roughening; and (ii) the slow bulk diffusion, D_b , simultaneously needed if monolayer interdiffusion through interfaces is to be avoided. Similarly, elemental semiconductors may be observed to require somewhat higher³ scaled growth temperatures $> T_m/2$. With the prevalence of research on semiconductors, and some ongoing effort also on metals, few studies of MBE growth in simple ionic systems have appeared, other than for fluorite structures grown on III-V semiconductors, on Si, or on silicides.⁴ This Letter reports new results for growth of alkali-halide (AH) crystals. These are the simplest of ionic solids, but their growth characteristics have remained little studied. We report homoepitaxy on cleaved single-crystal substrates, and heteroepitaxy also, including the growth of metastable disordered AH alloys. The results are of special interest for their universal characteristics and because the behavior, which is dominated by ledge and terrace properties, differs strikingly from that of metals and elemental semiconductors. The considerable extent to which growth behavior can differ among types of materials is thereby made apparent.

For the alkali metals, M , and halogens, X , the diatomic molecule MX is so strongly bound ($\sim 5 \text{ eV}$) that all kinetics of AH growth are dominated by motion of the ionic molecule.⁵ The interaction between AH (100) surfaces and the vapor phase at high temperature has been the subject of several investigations.⁶⁻⁸ Of particular interest are the energetics of molecular binding to ledges⁷ and the nucleation of new holes in perfect [100] terraces, with or without the promoting effects of impurities.^{6,8} Calculations by Hove⁹ for KCl explain why the

ionic molecule and the separate ions, M^+ and X^- , all bond quite weakly to [100] terraces. A large cohesion $\sim 1.5 \text{ eV}$ occurs when molecules diffusing on the terraces reach binding sites at the ledges (Fig. 1). This represents most of the increment between the Coulomb energy of the molecule and the Madelung energy of the crystal. Hove's calculations suggest that the separate ions have low activation energies $\sim 0.23 \text{ eV}$ on the terraces and, while explicit calculations are lacking, it is expected that the dominant molecular species exhibits a high mobility also. These factors have been investigated experimentally in the present research by methods we now describe.

Crystal growth took place in an MBE chamber equipped with several AH effusion cell sources, and with reflection high-energy electron diffraction (RHEED) and mass spectrometric characterization. The nominal substrate temperature could be varied from 1200 to 120 K by resistive heating or liquid-nitrogen cooling. The pyrolytic-boron-nitride (PBN) crucibles were isolated from the charges by a tantalum liner fixed to stainless-steel sleeves that extended into the MBE chamber to define the beam spread of the reactive AH species involved. These proved thermally sluggish but provided good stability over extended periods, once equilibrated. The deposition was monitored using two quartz crystals, with controlled rates from 0.1 to 100 $\text{\AA}/\text{sec}$ achieved.

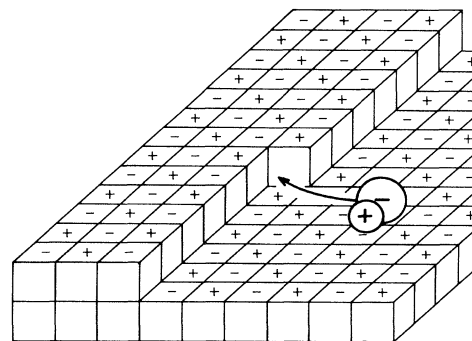


FIG. 1. Sketch of rocksalt [100] terraces, with a ledge to which molecular species bond strongly.

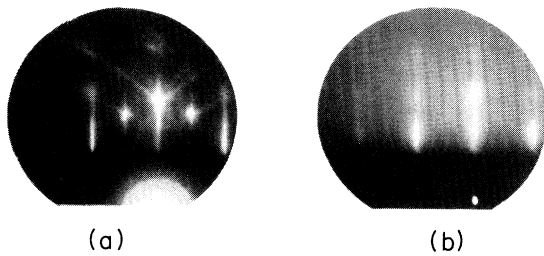


FIG. 2. [001] RHEED patterns of (a) cleaved and evaporated NaCl after 200-Å regrowth at 300 K, and (b) a metastable $\text{KCl}_{0.5}\text{I}_{0.5}$ alloy grown on KBr at 170 K.

Trimers, dimers, and monomers of M^+X^- were observed in the mass spectrum, generally fragmented by the ionizer,¹⁰ so that the dominant M^+X^- monomer in the molecular beam was observed mainly as an increase of M and X above their high background levels. This made the crystal monitor essential. The bell jar pressure normally reached the high 10^{-10} -Torr range.

Substrates were prepared for growth by cleaving the selected salt on a (100) plane, typically $1 \times 1 \text{ cm}^2$. When heated to $\sim 0.65T_m$ in the MBE chamber the crystal surfaces evaporated away at significant rates, with a resulting improvement of surface quality. Care was required with RHEED analysis because the electron beam damages AH surfaces, which desorb, most probably by Auger mechanisms.¹¹ The ability to evaporate an epitaxial structure away after study is an obvious convenience, permitting multiple uses of each substrate.

Smooth epitaxial regrowth from the molecular beam took place readily in most cases for a range of temperature below $0.5T_m$. Figure 2(a) shows a good RHEED pattern from 200 Å of regrown NaCl. It is of considerable interest that smooth regrowth at rates $> 10 \text{ Å/sec}$ continued at temperatures down to -150°C at which substrate cooling reached its limit. We have established that this nominal T_g is not in serious error owing to radiant heat from the source (the crystal was In soldered to the Cu base plate of the substrate holder, and the growth behavior was found to be independent of cell temperature and thermal shielding). Crystals of NaCl, NaBr, NaI, KCl, KBr, KI, RbCl, and RbI were grown under these conditions. By way of example, Fig. 3 shows reasonably good RHEED spectra taken along [001] and [011] for KBr grown 2 μm thick, mainly at a rate above 50 Å/sec on a substrate held near -150°C . We conclude that growth on AH (100) surfaces can take place rapidly at $T_g = 0.11T_m$. This corresponds to mobility with a typical activation energy $E_m \lesssim 0.1 \text{ eV}$ for the ionic molecule on [100] terraces (see below).

New results that have been obtained in three related areas during our studies will now be summarized. They pertain to heteroepitaxy and to the occurrence of metastable alloys and compounds stabilized by epitaxy. As alkali halides span a wide range of lattice constants,

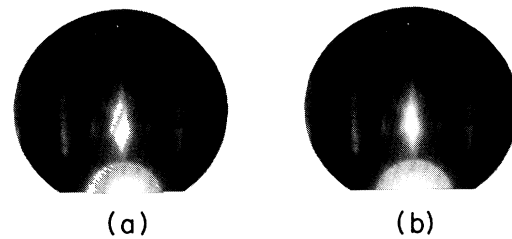


FIG. 3. RHEED patterns for (a) [001] and (b) [011] orientations of KBr 2 μm thick grown at $\geq 50 \text{ Å/sec}$ at $T_g \approx 120 \text{ K}$.

heteroepitaxy generally takes place with large misfits. We observe, accordingly, that when a second AH is grown on a foreign AH surface, the pseudomorphically strained state generally persists only for a few layers. Thereafter, however, the epitaxial material may grow as smooth (100) planes accurately oriented with the [001] directions of the substrate. Exceptions occurred for fluorides on nonfluorides, which did not grow well. We believe that in more favored cases the ledges of the substrate (Fig. 1) may, in effect, define the epilayer orientation, with the weak bonding between the two (100) cleavage planes otherwise generally relaxed. The crystal quality may be assessed from the x-ray Bragg scan of a thick KBr film grown on NaCl, shown in Fig. 4(a), where the clear $\text{Cu } K\alpha_1\text{-}K\alpha_2$ splitting of the substrate line remains partly visible for the KBr epilayer also. The corresponding structural coherence extends over $\sim 10^3 \text{ Å}$. By way of further illustration, Fig. 4(b) shows a scan of KI and KCl films grown successively on a KBr thin film, with comparable coherence retained throughout the sequence.

When two immiscible alkali halides are deposited together on a suitably lattice-matched substrate, we ob-

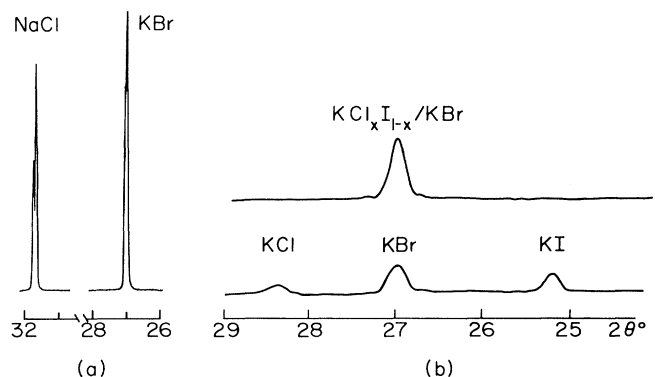


FIG. 4. (a) X-ray Bragg scans of NaCl substrate and thick KBr epilayer showing coherence lengths $\sim 10^3 \text{ Å}$. (b) X-ray Bragg scans for KCl (500 Å) and KI (600 Å) films grown on a KBr thin film (below) and for the metastable disordered $\text{KCl}_x\text{I}_{1-x}$ (1100 Å) alloy (above) grown on a KBr film [see Fig. 2(b) for RHEED].

serve by x-ray methods for high growth temperatures that they segregate in oriented columnar growths of the pure components, $\lesssim 100 \text{ \AA}$ wide. Using low substrate temperatures, however, we have been able to grow single-crystal metastable disordered AH alloys near $x = 0.5$, such as $\text{KCl}_x\text{I}_{1-x}$, which do not exist on the bulk phase diagram; they are stabilized epitaxially by forced atomic registry with the substrate in a manner predicted earlier,¹² and entirely analogous to semiconducting systems such as $\text{GaAs}_x\text{Sb}_{1-x}$.¹³ An x-ray Bragg scan of $\text{KCl}_{0.5}\text{I}_{0.5}$ grown on a KBr film is shown in Fig. 4(b), and its RHEED pattern in Fig. 2(b). Use of thin-film substrates for this purpose is essential, as the alloy Bragg peak would otherwise be overwhelmed by the substrate reflection. The new ordered compounds, such as NaRbCl_2 , that are also predicted to form by epitaxial stabilization¹² have not yet been observed in our experiments, despite protracted efforts to detect them.

We interpret the growth characteristics described above as arising mainly from weak molecular binding to [100] terraces, combined with strong cohesion at ledges. These features are evident in Fig. 5, where the overall energetics of the KCl system⁹ are sketched. The energies shown there must scale from one AH to the next in a "universal" form, as they are largely Coulomb energies defined by the core radii. Our results establish that the small E_m of molecules on terraces is also common to all systems studied. By way of explanation we note that the electrostatic potential $V(r)$ satisfies Laplace's equation outside the crystal surface, and a Fourier component of charge $\exp(i\mathbf{q}\cdot\mathbf{x})$ in the surface plane therefore gives rise to an exponential decay $V(r) \sim \exp[i\mathbf{q}\cdot\mathbf{x} - |q|z]$ with distance z outside the surface. This exponential weakening of the corrugated potential causes the observed high surface mobility.⁹ At the same time, molecules that reach the ledges at low growth temperatures

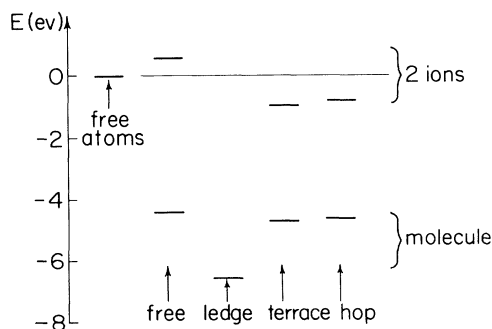


FIG. 5. Energetics of separated K^+ and Cl^- ion (top) and KCl molecules (bottom), free (column 2), in the crystal (i.e., on ledge, column 3), on a terrace (column 4), and activated during surface migration (column 5). Column 1 shows the energy zero as K and Cl neutral atoms. Columns 4 and 5 for ions differ by the calculated K^+ activation energy of 0.23 eV (Ref. 9).

are frozen into the growing terraces by the strong ledge bonding, and metastable alloys may thus form. This is not the case for ordered compounds, which require detailed kinetic balance to create order with small ordering energies. We suggest that the bonding to the ledge is so large at ~ 1.5 eV that the ordering energy difference (~ 0.1 eV predicted) may be too small for the ordering process to occur with significant probability during the kinetics of terrace diffusion to the ledges at the growth temperature. In fact the energy span of ledge bonding (~ 1.5 eV), molecular mobility (~ 0.1 eV), and ordering energy (~ 0.1 eV) makes it unlikely that these novel low-energy ordered arrangements may ever be achieved directly by MBE.

The resulting universal growth behavior of these salts may be displayed and contrasted with that of metals by means of particular diagram² that shows D_b and D_s as functions of T_m/T , as in Fig. 6. Values of D_b are known in several cases for $T > 0.7T_m$, both for anions and cations.¹⁴ With some scatter, the behavior averages as shown to a bulk diffusion that is a little slower than the well-known universal form (i.e., corresponding states relative to T_m) for metals. For all cases of surface diffusion on smooth terraces the preexponential is expected to be $\sim 10^{-3} \text{ cm}^2/\text{sec}$ from a simple combination of atomic jump distances and vibrational frequencies.¹⁵ The activation energies are roughly determined² by the observation that RHEED oscillations become rapidly damped for $D_s \lesssim 10^{-15} \text{ cm}^2/\text{sec}$, when insufficient mobility remains to smooth the surface before it is covered at growth rates $\sim 0.1 \text{ \AA}/\text{sec}$. For metals this typically occurs above $0.1T_m$ and for Si and Ge, above $0.2T_m$;¹⁶ the case of elemental semiconductors is also included for comparison in Fig. 6 and will be discussed elsewhere by one of us (C.P.F.). It is further known² that growth of smooth sharp interfaces with terraces 10^3 – 10^2 atoms wide requires $D_s \sim 10^{-7}$ – $10^{-8} \text{ cm}^2/\text{sec}$, otherwise nucleation of new ledges can occur, with consequent roughening. For metals and semiconductors these constructions reproduce in a satisfactory way the known lowest growth temperatures of $\sim 3T_m/8$ and $\sim 0.55T_m$, respectively (arrows in Fig. 6). For alkali halides, with $T_g \lesssim 0.1T_m$, the situation differs markedly. The necessary construction of D_s in Fig. 6 indicates an activation energy ~ 0.1 eV for molecular mobility on a surface terrace. This conclusion agrees well with semiempirical arguments advanced earlier.⁷ The breadth of different growth behavior indicated for the different crystal types in Fig. 6 appears firmly established.

In summary, we have shown that MBE growth of alkali halides has distinct universal characteristics that differ markedly from those of metals (and of elemental semiconductors) for reasons that can be identified clearly with the type of bonding. Particularly important are the weak binding of molecules to terraces and their strong bonding at ledges. The recognition of such universal patterns, and their considerable variation among crystal

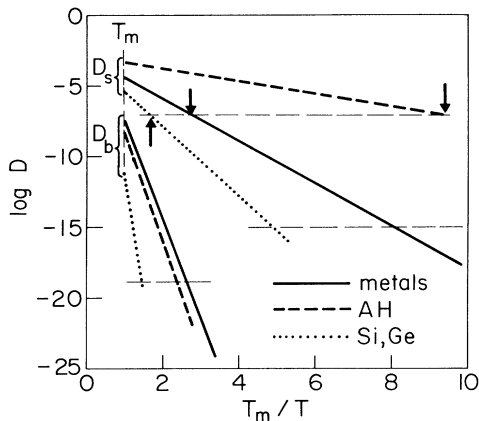


FIG. 6. Diagram showing deduced global dependences of surface and bulk diffusion coefficients, D_s and D_b , on T_m/T for metals (solid lines), elemental semiconductors (dotted lines), and salts (dashed lines). The construction is described in the text. Smooth flat interfaces generally require $D_s \gtrsim 10^{-8}-10^{-7}$ cm^2/sec , which fixes the lowest growth temperatures (arrows) as $\sim 3T_m/8$, $0.55T_m$, and $0.1T_m$ in the three cases. RHEED oscillations are expected for $D_s \gtrsim 10^{-15}$ cm^2/sec and bulk interdiffusion for $D_b \gtrsim 10^{-19}$ cm^2/sec .

types, is an important goal in the global understanding of growth behavior. In further studies we have found that heteroepitaxy can often yield excellent AH overlayers with incommensurate but aligned relaxed lattices, having a large misfit. Epitaxially stabilized disordered AH alloys may be created, but not ordered compounds, probably because the bonding of the ionic molecule to the ledges is large compared to the ordering energy.

We thank M. V. Klein for generously providing single-crystal substrates. This research was supported in

part by the Department of Energy under Contract No. DE-AC02-76ER01198.

¹J. E. Cunningham, J. A. Dura, and C. P. Flynn, in *Metallic Multilayers and Epitaxy*, edited by M. Hong *et al.* (The Metallurgical Society, Warrendale, PA, 1988), p. 77.

²C. P. Flynn, *J. Phys. F* **18**, L195 (1988).

³Lower limits of growth are approximately as follows: For Si, 900 K [$\sim 0.54T_m$, see, e.g., H. P. Zeindl *et al.*, in *Molecular Beam Epitaxy*, edited by C. T. Foxon and J. J. Harris (North-Holland, Amsterdam, 1987)] and for Ge, 600 K ($\sim 0.5T_m$, see, e.g., Y. Fukada and Y. Kohama, *ibid.*).

⁴See, e.g., P. W. Sullivan, *Appl. Phys. Lett.* **44**, 190 (1984), and several helpful papers in Ref. 3.

⁵Listed by J. A. Kerr, in *CRC Handbook of Physics and Chemistry*, edited by Robert C. Weast (CRC Press, Boca Raton, FL, 1988), 69th ed., p. F174.

⁶B. J. Stein and H. J. Meyer, *J. Cryst. Growth* **49**, 696 (1980).

⁷R. B. Bjorklund and K. G. Spears, *J. Chem. Phys.* **66**, 3448 (1977); **66**, 3437 (1977).

⁸W. Laaser, H. Dabringhaus, and H. J. Meyer, *J. Cryst. Growth* **62**, 248 (1983).

⁹J. E. Hove, *Phys. Rev.* **99**, 430 (1955).

¹⁰See, e.g., L. Friedman, *J. Chem. Phys.* **23**, 477 (1955).

¹¹P. Williams and G. Gillen, *Surf. Sci.* **180**, L109 (1987).

¹²C. P. Flynn, *Phys. Rev. Lett.* **57**, 599 (1986).

¹³H. R. Jen, Y. T. Cherg, and G. B. Stringfellow, *Appl. Phys. Lett.* **48**, 1603 (1986).

¹⁴For D_b see, e.g., C. P. Flynn, *Point Defects and Diffusion* (Oxford Univ. Press, Oxford, 1972).

¹⁵This is established for metal by S. C. Wang and G. Ehrlich, *Surf. Sci.* (to be published).

¹⁶RHEED oscillations die out quickly for Si and Ge (111) near 300 K; see J. Aarts and P. K. Larson, *Surf. Sci.* **188**, 391 (1987).

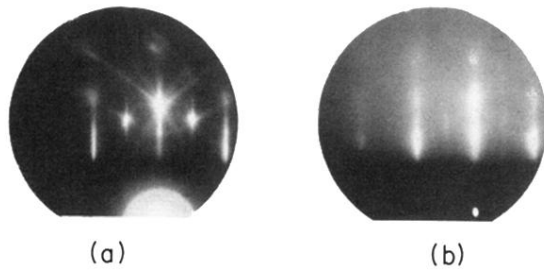


FIG. 2. [001] RHEED patterns of (a) cleaved and evaporated NaCl after 200-Å regrowth at 300 K, and (b) a metastable $\text{KCl}_{0.5}\text{I}_{0.5}$ alloy grown on KBr at 170 K.

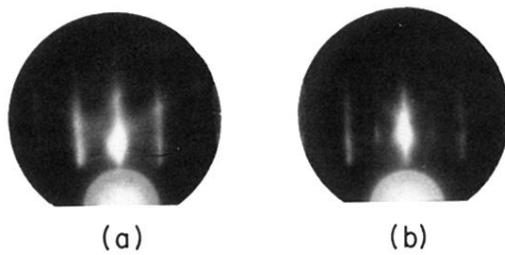


FIG. 3. RHEED patterns for (a) [001] and (b) [011] orientations of KBr $2\ \mu\text{m}$ thick grown at $\approx 50\ \text{\AA}/\text{sec}$ at $T_g \approx 120\ \text{K}$.